

# On the discharging process of titanium-based hydrogen storage alloy electrode via a.c. impedance analysis

B. Luan, H. Zhao, H.K. Liu, S.X. Dou

*Institute for Materials Technology and Manufacturing, University of Wollongong, Northfields Avenue, Wollongong, NSW 2522, Australia*

Received 22 January 1996; revised 29 February 1996; accepted 7 March 1996

## Abstract

An a.c. impedance technique is applied to study the frequency response during the discharging process of an electrode fabricated from titanium-based hydrogen storage alloy. Conditions are discussed under which either diffusion or adsorption of hydrogen control the overall electrode process. The impedance spectra obtained at different discharge states of the electrode reveal that the rate-determining-step (RDS) of the discharging process varies from an electrochemical process to diffusion of hydrogen along with the discharging of the electrode. The impedance spectra obtained at different temperatures of discharging also show a significant variation of RDS. A further understanding of the discharging process of titanium-based hydrogen storage alloy electrode is discussed.

**Keywords:** Titanium; Hydrogen storage; Electrodes; Impedance

## 1. Introduction

Development of rechargeable nickel/metal-hydride batteries with titanium-based hydrogen storage alloy anodes remains a major challenge for those involved in the research and development of batteries with high specific energies. A series of studies on the performance of titanium-based hydrogen storage alloy electrode has been carried out previously by the authors [1–5]. These reports have revealed new understanding of elemental substitutions, surface modifications of the alloy powder, and the mechanism of capacity decay of the electrode during charge/discharge cycling. In other work, the authors [6] have formulated a novel electrochemical discharge model for the discharge process of the electrode. This model is based on the results of X-ray diffraction (XRD) analysis and a.c. spectroscopy, as well as theoretical calculations.

The a.c. impedance technique is a powerful means for in situ analysis of processes such as corrosion, polymer formation, electropolishing and battery reactions. The wide continuous frequency range available permits investigation of surface processes that differ widely in relaxation times. Furthermore, the simple forms of the perturbation and response function render the mathematical analysis of complex reaction mechanisms relatively simple. Provided that the amplitude of the perturbation potential is sufficiently small, the components of the impedance at an electrode/electrolyte

interface can be regarded as linear, that is, the impedance of the individual components are independent of potential. Accordingly, the interface may be represented by an equivalent electrical circuit that consists of linear components only.

Impedance spectroscopy has been used to study a wide variety of electrochemical systems: for such systems, the charge transfer involved at an interface between an electrode and an electrolyte occurs via a succession of elementary phenomena that are more or less strongly coupled, namely: (i) transport of the reacting species; (ii) adsorption of reacting species on the electrode, and (iii) chemical and electrochemical interfacial reactions, that often occur in several mono-electronic steps. To date, the most significant results have been obtained by measurement of the electrochemical impedance which leads to kinetic characterization of the phenomena in terms of process rates (mass transport, adsorption, electrochemical or chemical reaction). As reported in our previous *in situ* a.c. impedance analysis [6], the discharge process of the Ti<sub>2</sub>Ni alloy electrode exposed to 6 M KOH solution is composed of the following steps: (i) chemical and electrochemical reactions on the surface of the electrode; (ii) diffusion of hydrogen from inside the electrode, and (iii) adsorption of hydrogen on the surface of the electrode. As all these processes are very temperature dependent and are closely related to the discharge state of the electrode, the main objectives of the research reported here are to study the influences of temperature and the electrode discharge state on the

discharge process of a  $\text{Ti}_2\text{Ni}$  electrode exposed to 6 M KOH aqueous solution, in order to understand more about the discharge kinetics.

## 2. Experimental

### 2.1. Electrode preparation and characterization

$\text{Ti}_2\text{Ni}$  alloy was made by vacuum arc melting under argon protection. Care was taken to avoid any metal evaporation. Homogeneity was ensured by melting both sides of the alloy ingots, alternately. The development of the  $\text{Ti}_2\text{Ni}$  phase was confirmed by XRD analysis. The alloy ingot was then crushed and ground into powder of below 100 mesh using a Planetary Mill Pulverisette 5. The fine powder was then mixed with 10 wt.% polyvinyl alcohol (PVA) at a ratio of 10:1. The mixture was casted onto a foam nickel sheet and, after drying, was pressed at a pressure of  $15 \text{ kN cm}^{-2}$ .

Discharging of the electrode was conducted galvanostatically at a current density of  $20 \text{ mA g}^{-1}$  in 6 M KOH aqueous solution in a divided cell. Platinum was employed as an auxiliary electrode and  $\text{Hg}/\text{HgO}$  (1 M NaOH) as a reference electrode. All potentials are reported with respect to this electrode.

Impedance analysis was carried out using Model 6310 Electrochemical Impedance Analyser interfaced with EIS 3.8 software supplied by Princeton Instruments. The amplitude of the sinusoidal wave was  $5 \text{ mV}$  to ensure a linear perturbation. The frequency range was  $10^3$  to  $10^{-2}$  Hz. The whole system is shown schematically in Fig. 1.

Studies of the influence of temperature and discharge state of the electrode were performed via the following procedures.

### 2.2. Temperature effects

Electrodes were fully charged and rested for 30 min until the electrode potential became steady ( $-0.97 \text{ V}$ ). The fully charged electrodes were then discharged galvanostatically ( $20 \text{ mA g}^{-1}$ ) at  $20$  and  $5^\circ\text{C}$ . Temperature accuracy was

ensured by placing the divided cell in a JULABO F10 water bath with internal thermometer monitoring. Impedance measurements were conducted during the discharging process at  $20$  and  $5^\circ\text{C}$ .

### 2.3. Influence of electrode discharge state

To study the influence of electrode discharge state on the electrochemical impedance response, impedance measurements were carried out at  $20^\circ\text{C}$  and starting at the electrode potentials of  $-0.97$ ,  $-0.84$  and  $-0.79 \text{ V}$  that correspond to the initial, medium and final discharge states of the electrode, respectively. The electrode was galvanostatically discharged simultaneously with impedance measurements.

## 3. Results and discussion

The electrode impedance spectra obtained at different temperatures and different states of discharge are given in Figs. 2–4.

### 3.1. Temperature effects

At  $20^\circ\text{C}$ , and at an electrode potential of  $-0.97 \text{ V}$ , there exists an inductive loop in the fourth quadrant and two consecutive capacitive loops in the first quadrant (see Fig. 2). At  $5^\circ\text{C}$  and an electrode potential of  $-0.97 \text{ V}$ , however, the

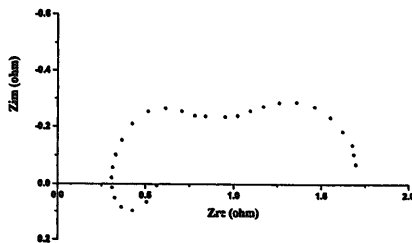


Fig. 2. Impedance spectrum obtained at  $20^\circ\text{C}$  during discharge with an electrode potential of  $-0.97 \text{ V}$ .

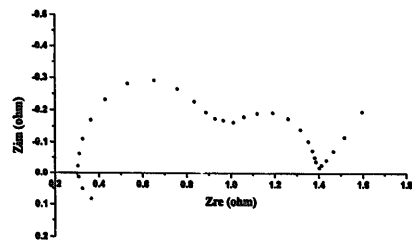


Fig. 3. Impedance spectrum obtained at  $5^\circ\text{C}$  during discharge process with an electrode potential of  $-0.97 \text{ V}$ .

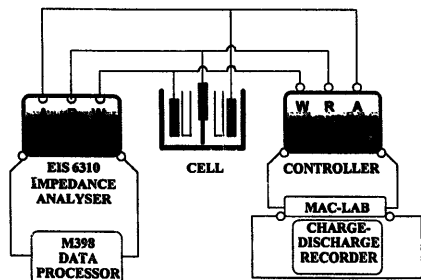


Fig. 1. Schematic of test system.

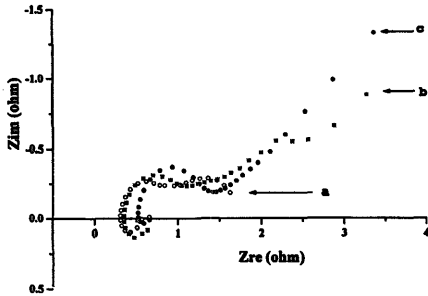


Fig. 4. Impedance spectrum obtained at different discharge states. (a) initial state ( $-0.97$  V); (b) medium state ( $-0.84$  V), and (c) final state ( $-0.79$  V).

impedance spectrum of the electrode changes to an inductive loop in the fourth quadrant and two consecutive loops in the first quadrant, but now followed a line of  $45^\circ$  slope, see Fig. 3.

It is generally believed that the first capacitive loop in the first quadrant corresponds to a Faradaic reaction, the second loop to adsorption, and the  $45^\circ$  Warburg slope to diffusion of the reactant. Previous work [6] revealed that, after a series of mathematical calculations based on impedance and XRD data, the first capacitive loop represents the main discharging process. This is the electrochemical reaction of atomic hydrogen. The second capacitive loop corresponds to the adsorption of hydrogen. The  $45^\circ$  slope relates to the diffusion of hydrogen from inside the hydrogen storage alloy. Finally, the inductive loop in the fourth quadrant relates to the adsorption of  $(\text{Ti}_2\text{NiOH})^-$ , an intermediate species in the oxidation of the  $\text{Ti}_2\text{Ni}$  alloy during the discharging process.

As the oxidation of the alloy is very slow compared with other electrode processes (otherwise, the alloy cannot be used reversibly), there exists three main steps during the discharging process: (i) diffusion of atomic hydrogen from inside the bulk alloy to the surface of the electrode; (ii) adsorption of atomic hydrogen on the surface of the electrode, and (iii) oxidation of atomic hydrogen which generates electric current. Thus, the discharge process of the electrode is determined by these three steps, as dictated by the variations of electrochemical and/or chemical conditions, e.g. the discharge state of the electrode and discharge temperature, as shown in Figs. 2–4.

As is shown in Figs. 2 and 3, the discharge process is diffusion controlled at  $5^\circ\text{C}$ , but the reaction (either electrochemical reaction or adsorption) controlled at  $20^\circ\text{C}$ . To identify the step that controls the discharging process at  $20^\circ\text{C}$ , the following discussion is essential.

According to the Nernst equation for an electrode process that involves adsorption, there exists the following relation [7]

$$i = nF \left[ k_f C_{\text{so}} \left( \frac{\Gamma_{\text{R}}^0 - \Gamma_{\text{R}}}{\Gamma_{\text{R}}^0} \right) \exp \left( -\frac{\alpha n F \varphi}{RT} \right) \right] \quad (1)$$

where  $i$  is the electrode reaction rate;  $\Gamma_{\text{R}}$  and  $C_{\text{so}}$  are the surface concentration of hydrogen at reduction and oxidation states, respectively;  $\Gamma_{\text{R}}^0$  is the maximum adsorption concentration of hydrogen;  $k_f$  is the rate constant of the forward electrochemical reaction ( $\text{H}_{\text{ads}} \rightarrow \text{H}^+ + e^-$ ). The remaining symbols have their normal meanings. From Eq. (1), when other conditions are kept constant, increase in temperature is beneficial to the electrochemical reaction. If this is the electrochemical reaction that controls the discharge process, then an increase in temperature should make diffusion become the rate-determining-step (RDS). This is obviously not the situation that gives the experimental results presented here. Therefore, it is reasonable to conclude that it is actually hydrogen adsorption that controls the discharging process at  $20^\circ\text{C}$ .

It is clear that there exists a transition of the RDS from diffusion to adsorption of hydrogen with elevation of the temperature from  $5$  to  $20^\circ\text{C}$ . The reason for this transition may be elucidated as follows.

It is commonly known that an increase in temperature will raise the energy of the adsorbed species and therefore, will reduce the stability of adsorption. Thus, increasing temperature is unfavourable to the adsorption process. Moreover, adsorption of a species must be exothermic if it is to proceed spontaneously [8]. The argument behind this statement is as follows. When a species is adsorbed on a surface, its translational freedom is reduced, and thus the process is accompanied by a decrease in entropy. Since  $\Delta G = \Delta H - T\Delta S$ , it follows that  $\Delta H$  must be negative for  $\Delta G$  to be negative, and a negative enthalpy change corresponds to an exothermic process. In addition, it is commonly known that the enthalpy change for physisorption is about  $-20 \text{ kJ mol}^{-1}$ , while for chemisorption  $\Delta H$  is usually more negative, i.e., about  $-200 \text{ kJ mol}^{-1}$ . This indicates an exothermal process. From the view of chemical equilibrium, it is generally known that a rise in temperature is detrimental to an exothermic process. Therefore, increasing temperature will reduce hydrogen adsorption.

On the other hand, increase in temperature is beneficial to dehydrogenating of the metal hydride ( $\text{Ti}_2\text{Ni-H}$ ) which leads to a more ready supply of hydrogen from inside the hydrogen storage alloy and, this, increases the gradient of thermodynamic chemical potential of hydrogen. As the chemical potential gradient of hydrogen is actually acting as the driving force for hydrogen diffusion, hydrogen transport is enhanced.

From the above discussion, it is believed that a temperature increase is beneficial to diffusion, but detrimental to the adsorption of hydrogen. In another words, the resistance of hydrogen adsorption increases with increasing temperature, while the resistance for hydrogen diffusion decreases. This is consistent with the experimental observations shown in Figs. 2 and 3. At  $20^\circ\text{C}$ , the Warburg for hydrogen adsorption is about  $850 \text{ m}\Omega$ , and a Warburg impedance is not observed.

Nevertheless, with lowering of the temperature down to 5 °C, the hydrogen adsorption loop (second loop in the first quadrant) shrinks and the adsorption resistance decreases to only 450 mΩ (i.e., about half of that at 20 °C) and there appears a Warburg impedance slope, see Fig. 2. This suggests that the diffusion of hydrogen from inside the bulk alloy now becomes the RDS and drastically reduces the discharge efficiency (the specific capacity of the Ti<sub>2</sub>Ni electrode at 5 °C is only about 55 mAh g<sup>-1</sup>, which is much smaller compared with the specific capacity of about 160 mAh g<sup>-1</sup> at 20 °C).

The equivalent circuits that correspond to the electrode discharged at 20 and 5 °C are shown in Fig. 5(a) and (b), respectively.

### 3.2. Influences of electrode discharge state

At the very initial stage of discharge when the electrode potential is -0.97 V, the impedance spectrum consists of an inductive loop in the fourth quadrant followed by two consecutive capacitive loops in the first quadrant, see curve (a) in Fig. 4.

At a medium state of discharge, i.e. when the electrode potential has fallen to -0.84 V, the impedance also consists of an inductive loop in the fourth quadrant and two consecutive capacitive loops in the first quadrant, but now followed by an emerging straight line, see curve (b) in Fig. 4.

At the final state of discharge, when the electrode potential has declined to -0.79 V (which as found in previous work [3–5], is close to the end of discharge), the impedance diagram changes to one capacitive loop and a typical line of 45° slope which is known as the Warburg impedance, refer curve (c) in Fig. 4. From curve (a) in Fig. 4, it is clear that, at the very initial stage of discharge, the impedance diagram consists of a Faradaic reaction loop and an adsorption loop in the first quadrant. The amount of hydrogen stored inside a fully charged hydrogen storage alloy electrode is sufficient to render hydrogen transport facile due to the high chemical poten-

tial of hydrogen. With further discharge of the electrode, however, the amount of hydrogen stored inside the bulk alloy decreases, and this results in a decrease in the chemical potential gradient of hydrogen. As mentioned above, the chemical potential gradient actually acts as the driving force for hydrogen diffusion out of the alloy; a decrease in hydrogen concentration will inevitably increase the transport resistance. This is evident from the appearance of the Warburg impedance, as shown in curve (b) in Fig. 4, which is indicative of a transition in the RDS from adsorption to diffusion of hydrogen. The discharge process at this stage may be controlled by both adsorption and diffusion of hydrogen.

As the electrode approaches the end of the entire discharge process, the adsorption loop shrinks further and disappears, but there is clearly a typical Warburg impedance, see curve (c) in Fig. 4. This can be attributed to an insufficient quantity of hydrogen inside the alloy which leads to a further increase in the resistance to hydrogen transport. Therefore, the amount of hydrogen atoms that diffuses out to the electrode/electrolyte interface cannot sustain the electrochemical reactions. In another words, the discharge process now becomes controlled by the diffusion of hydrogen.

One of our experimental observations is consistent with the above discussion. It is observed that the electrode potential drop becomes much faster at the end of discharge than at either the beginning or the middle of discharge. This may now be explained as follows. Since the process is actually controlled by the diffusion of hydrogen at the end of discharge, there is insufficient hydrogen at the electrode/electrolyte interface. Since the electrode is discharged galvanostatically (which acts as an 'electron pump'), the majority of the current applied is now used for the polarization of

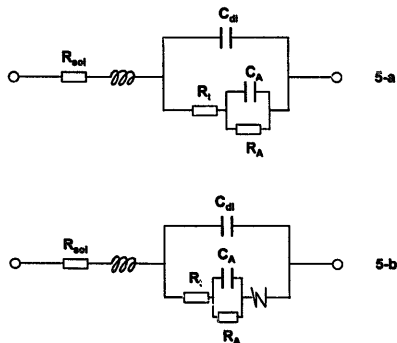


Fig. 5. Equivalent circuits that correspond to electrode discharged at: (a) 20 °C (corresponding to Fig. 2), and (b) 5 °C (corresponding to Fig. 3).

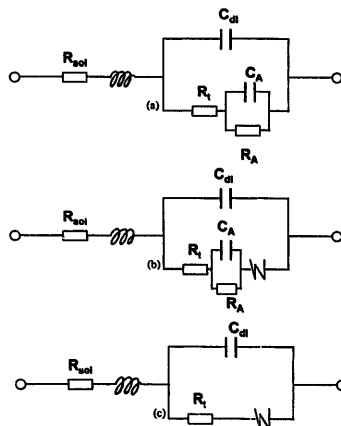


Fig. 6. Equivalent circuits that correspond to electrode discharged at: (a) initial state (corresponding to Fig. 4(a)); (b) medium state (corresponding to Fig. 4(b)), and (c) final state (corresponding to Fig. 4(c)).

the electrode, and not for the electrochemical oxidation of hydrogen on the surface of the electrode. Consequently, this gives a much faster drop in electrode potential.

Based on the above discussion, the equivalent circuits that correspond to the initial, medium and final states of the discharging process are given in Fig. 6(a)–(c), respectively.

Rubinstein [9] has stated that the structure and composition, as well as the chemical and electrochemical reactivities, of the adsorbed atomic, ionic and molecular layers are influenced by the electrode potential, temperature, solution pH, adsorbate concentration, crystallographic structure and composition of the electrode surface, as well as, in the case of molecular adsorption, by molecular structure of the adsorbate. The findings of the present work indicate clearly that the influence of electrode potential (discharge state) and temperature on the adsorption of hydrogen are in agreement with Rubinstein's point of view.

#### 4. Conclusions

The following conclusions can be drawn from impedance measurements on titanium-based hydrogen storage alloy electrodes.

1. Temperature increase is beneficial to the dehydrogenation of  $Ti_2NiH$  and, therefore, to the diffusion of hydrogen. By contrast, it is detrimental to the adsorption of hydrogen on the surface of the electrode. The RDS of the discharge process can be changed from diffusion to adsorption of hydrogen with elevation of the discharge temperature.

2. The discharge state of the electrode influences the discharge kinetics of the electrode. For a fully charged electrode,

diffusion of hydrogen is fast and adsorption is the RDS. At a medium state-of-discharge, the process may be controlled by the combination of diffusion and adsorption of hydrogen. At the end of discharge, however, there exists an inadequate hydrogen supply from inside the hydrogen storage alloy. Diffusion of hydrogen now becomes the RDS and controls the whole discharge process.

#### Acknowledgements

The authors are grateful for the scholarship provided to Benli Luan by AUSAID.

#### References

- [1] B. Luan, N. Cui, H. Zhao, H.K. Liu and S.X. Dou, *J. Power Sources*, 52 (1994) 295–299.
- [2] B. Luan, N. Cui, H. Zhao, H.K. Liu and S.X. Dou, *J. Power Sources*, 55 (1995) 101–106.
- [3] B. Luan, N. Cui, H. Zhao, H.K. Liu and S.X. Dou, *J. Power Sources*, 55 (1995) 197–203.
- [4] B. Luan, N. Cui, H. Zhao, H.K. Liu and S.X. Dou, *Int. J. Hydrogen Energy*, in press.
- [5] B. Luan, N. Cui, H. Zhao, S. Zhong, H.K. Liu and S.X. Dou, *J. Alloys Comp.*, 233 (1996) 230.
- [6] B. Luan, H. Zhao, H.K. Liu and S.X. Dou, *J. Electrochem. Soc.*, in press.
- [7] S.W. Tian, *Transient Techniques of Electrochemistry*, Scientific Publisher, Beijing, 1994, p. 305.
- [8] P.W. Atkins, *Physical Chemistry*, Oxford University Press, London, 1978, pp. 937–953.
- [9] I. Rubinstein, *Physical Electrochemistry*, Marcel Dekker, New York, 1995, pp. 469–514.